Nonmagnetic impurity effects in MgB_2

Koichi Watanabe and Takafumi Kita
Division of Physics, Hokkaido University, Sapporo 060-0810, Japan
(Dated: February 2, 2008)

We study nonmagnetic impurity effects in MgB_2 using the quasiclassical equations of superconductivity for a weak-coupling two-band model. Parameters in the model are fixed so as to reproduce experiments on MgB_2 as closely as possible. The quasiparticle density of states and the specific heat are calculated for various values of the interband impurity scattering. The density of states changes gradually from a two-gap structure into the conventional single-gap structure as the interband scattering increases. It is found that the excitation threshold is not a monotonic function of the interband scattering. Calculated results for the specific heat are in good agreements with experiments on samples after irradiation.

PACS numbers: Valid PACS appear here

I. INTRODUCTION

Superconductivity in MgB_2 has attracted much attention since its discovery by Nagamatsu *et al.*[1] Besides its high transition temperature $T_c \cong 40K$ for a phonon-mediated pairing mechanism,[2] it has a striking novel feature that approximately two different energy gaps open on different pieces of the Fermi surface. Accompanied with theoretical predictions,[3,4,5,6] this multigap structure has been established within a short period by specific heat experiments,[7,8,9,10,11,12,13] point-contact spectroscopy,[14,15,16] and scanning tunneling microscope.[17,18,19] The larger gap opens on cylindrical Fermi surfaces of the σ-band with $2\Delta_\sigma(0)/k_BT_c = 3.6 - 4.5$, whereas the smaller one has the size $2\Delta_\pi(0)/k_BT_c = 1.1 - 1.5$ on three dimensional Fermi surfaces of the π-band.

Impurity effects of this material are very interesting to study. According to Anderson's theorem for classic s-wave superconductors,[20,21] nonmagnetic impurities do not affect superconducting properties in zero magnetic field. However, it was shown later by Markowitz and Kadanoff[22] that T_c is actually reduced in the presence of gap anisotropy and impurity scattering. An application to a two-band model is due to Golubov and Mazin.[23] Indeed, they predicted a rather drastic decrease of T_c due to the interband impurity scattering. They also found that, as the interband scattering increases, the density of states changes from the two-gap structure inherent to the two-band model to the conventional single-gap structure. This reduction of T_c has been confirmed recently by a couple of experiments. Wang *et al.*[13] measured the specific heat of polycrystalline MgB_2 after irradiation. They found both suppression of T_c and a tendency towards a single-gap structure as the scattering is increased by irradiation. Lee *et al.*[24] clarified the possibility of complete suppression of superconductivity by replacing B in MgB_2 by C. However, few quantitative calculations have been performed on the impurity effects based on a realistic model for MgB_2.[25] For example, the specific heat has been calculated by Choi *et al.*[4] and Golubov *et al.*[12] based on the clean-limit Eliashberg equation to obtain excellent quantitative agreements. However, no detail study has been performed for the specific heat from clean to dirty limits based on a microscopic model.

With these observation, we investigate nonmagnetic impurity effects in MgB_2. We thereby clarify impurity-concentration dependence of the quasiparticle density of states and the specific heat, choosing the parameters in the model suitable for MgB_2. Section II gives the formulation. Section III presents calculated results. Section IV summarizes the paper. We put $\hbar = k_B = 1$ throughout.

II. FORMULATION

A. Quasiclassical equations

We start from the Eilenberger equations[26] for the Suhl-Matthias-Walker model[27] with impurities, which form one of the most convenient frameworks to study impurity effects of the two-band model. We here adopt the formulation on the real energy axis instead of using Matsubara frequencies, which has an advantage that the free-energy functional can be defined unambiguously.

The Eilenberger equation on the real energy axis is given for the uniform case by

$$\left(-i\varepsilon + \sum_\beta \frac{\langle g_\beta^{\rm R}\rangle}{2\tau_{\alpha\beta}}\right) f_\alpha^{\rm R} = \left(\Delta_\alpha + \sum_\beta \frac{\langle f_\beta^{\rm R}\rangle}{2\tau_{\alpha\beta}}\right) g_\alpha^{\rm R} \,. \quad (1)$$

Here $f_\alpha^{\rm R} \equiv f_\alpha^{\rm R}(\varepsilon, \mathbf{k}_{\rm F})$ and $g_\alpha^{\rm R} \equiv g_\alpha^{\rm R}(\varepsilon, \mathbf{k}_{\rm F})$ are retarded quasiclassical Green's functions specified by the band index α $(= \sigma, \pi)$ and the Fermi wave vector $\mathbf{k}_{\rm F}$. They are connected by $g_\alpha^{\rm R} = (1 - f_\alpha^{\rm R} f_\alpha^{\rm R\dagger})^{1/2}$ with $f_\alpha^{\rm R\dagger}(\epsilon, \mathbf{k}_{\rm F}) = f_\alpha^{\rm R*}(-\epsilon, -\mathbf{k}_{\rm F})$. The symbol $\langle \cdots \rangle$ denotes the average over the Fermi surface for the relevant band with $\langle 1 \rangle = 1$. The quantity $\tau_{\alpha\beta}$ is the relaxation time for the nonmagnetic impurity scattering from α- to β-band; they satisfy $\frac{1}{\tau_{\alpha\beta}} = \frac{N_\beta(0)}{N_\alpha(0)} \frac{1}{\tau_{\beta\alpha}}$, where $N_\alpha(0)$ is the normal-state density of states at the Fermi energy for the α-band. Finally, Δ_α

is determined self-consistently by

$$\Delta_\alpha = \sum_\beta \frac{\lambda_{\alpha\beta}}{2i} \int_{-\varepsilon_c}^{\varepsilon_c} d\varepsilon \phi(\varepsilon) \langle f_\beta^{\rm R}(\varepsilon, \mathbf{k}_{\rm F}) \rangle \,, \tag{2}$$

where ε_c is the cutoff energy, $\phi(\varepsilon) \equiv \tanh(\varepsilon/2T)$, and $\lambda_{\alpha\beta}$ is dimensionless coupling constant with $\lambda_{\alpha\beta} = \frac{N_\beta(0)}{N_\alpha(0)} \lambda_{\beta\alpha}$.

The functional for the free-energy difference corresponding to Eqs. (1) and (2) are given by

$$\begin{aligned}
&F_s - F_n \\
&= \sum_{\alpha(\neq\beta)} N_\alpha(0) \Bigg\{ \frac{|\Delta_\alpha|^2}{\lambda_{\alpha\alpha}} - \frac{1}{2i} \int_{-\varepsilon_c}^{\varepsilon_c} d\varepsilon \phi(\varepsilon) \langle I_\alpha(\varepsilon) \rangle \\
&\quad - \frac{\lambda_{\alpha\beta}}{\lambda_{\alpha\alpha}} \frac{1}{2i} \int_{-\varepsilon_c}^{\varepsilon_c} d\varepsilon \phi(\varepsilon) \Big[\Delta_\alpha^* \langle f_\beta^{\rm R}(\varepsilon) \rangle + \Delta_\alpha \langle f_\beta^{\rm R\dagger}(\varepsilon) \rangle \Big] \\
&\quad + \frac{1}{(2i)^2} \int_{-\varepsilon_c}^{\varepsilon_c} \int_{-\varepsilon_c}^{\varepsilon_c} d\varepsilon d\varepsilon' \phi(\varepsilon) \phi(\varepsilon') \\
&\qquad \times \Big[\frac{\lambda_{\alpha\beta}^2}{\lambda_{\alpha\alpha}} \langle f_\beta^{\rm R\dagger}(\varepsilon) \rangle \langle f_\beta^{\rm R}(\varepsilon') \rangle + \lambda_{\alpha\beta} \langle f_\beta^{\rm R\dagger}(\varepsilon) \rangle \langle f_\alpha^{\rm R}(\varepsilon') \rangle \Big] \\
&\quad - \frac{1}{2i} \int_{-\varepsilon_c}^{\varepsilon_c} d\varepsilon \phi(\varepsilon) \\
&\qquad \times \Big[\frac{\langle f_\alpha^{\rm R\dagger}(\varepsilon) \rangle \langle f_\beta^{\rm R}(\varepsilon) \rangle + \langle g_\alpha^{\rm R}(\varepsilon) \rangle \langle g_\beta^{\rm R}(\varepsilon) \rangle - 1}{2\tau_{\alpha\beta}} \Big] \Bigg\} \,,
\end{aligned} \tag{3}$$

with

$$\begin{aligned}
I_\alpha &= \Delta_\alpha^* f_\alpha^{\rm R} + \Delta_\alpha f_\alpha^{\rm R\dagger} - 2i\varepsilon(g_\alpha^{\rm R} - 1) \\
&\quad + \frac{f_\alpha^{\rm R} \langle f_\alpha^{\rm R\dagger} \rangle + \langle f_\alpha^{\rm R} \rangle f_\alpha^{\rm R\dagger}}{4\tau_{\alpha\alpha}} + \frac{g_\alpha^{\rm R} \langle g_\alpha^{\rm R} \rangle - 1}{2\tau_{\alpha\alpha}} \,.
\end{aligned} \tag{4}$$

Equation (3) is a direct extension of Eilenberger's free-energy functional[26] to the two-band model. Indeed, variations of $F_s - F_n$ with respect to $f_\alpha^{\rm R\dagger}$ and Δ_α^* lead to Eqs. (1) and (2), respectively.

The entropy is obtained from this free-energy functional by $S_s = S_n - \partial(F_s - F_n)/\partial T$. Noting the stationarity of $F_s - F_n$ with respect to $f_\alpha^{\rm R\dagger}$ and Δ_α^*, we only have to differentiate with respect to the explicit temperature dependence in $\phi(\epsilon) = \tanh(\epsilon/2T)$. We thereby obtain an explicit analytic expression for the entropy as

$$\begin{aligned}
S_s = S_n + \sum_{\alpha(\neq\beta)} N_\alpha(0) \frac{1}{2i} \int_{-\varepsilon_c}^{\varepsilon_c} d\varepsilon \frac{\partial \phi(\varepsilon)}{\partial T} \Bigg\{ \langle I_\alpha(\varepsilon) \rangle \\
+ \frac{\langle f_\alpha^{\rm R\dagger}(\varepsilon) \rangle \langle f_\beta^{\rm R}(\varepsilon) \rangle + \langle g_\alpha^{\rm R}(\varepsilon) \rangle \langle g_\beta^{\rm R}(\varepsilon) \rangle - 1}{2\tau_{\alpha\beta}} \Bigg\} \,.
\end{aligned} \tag{5}$$

In deriving this expression, we have used Eq. (2). Finally, the specific heat is calculated by numerically differentiating Eq. (5) as

$$C_s = C_n + T \frac{d(S_s - S_n)}{dT} \,. \tag{6}$$

Equations (5) and (6) form a convenient and efficient starting point to calculate the specific heat for various impurity concentrations.

There is a disadvantage in the coupled self-consistency equations (1) and (2) that they may not be very stable numerically. However, it can be removed when ε_c is much larger than both Δ_α and $1/\tau_{\alpha\beta}$. This condition is well satisfied in MgB_2 where ε_c corresponds to the Debye energy $\omega_{\rm D} \sim 1000K$.[8] Then using the asymptotic property $f_\alpha^{\rm R} \to \Delta_\alpha/(-i\varepsilon)$ as $|\varepsilon| \to \infty$, Eq. (2) is transformed as

$$\begin{aligned}
\Delta_\alpha &= \sum_\beta \frac{\lambda_{\alpha\beta}}{2i} \int_{-\varepsilon_c}^{\varepsilon_c} d\varepsilon \phi(\varepsilon) \Big[\langle f_\beta^{\rm R}(\varepsilon, \mathbf{k}_{\rm F}) \rangle - \frac{\Delta_\beta}{-i\varepsilon} \Big] \\
&\quad + \sum_\beta \frac{\lambda_{\alpha\beta}}{2} \int_{-\varepsilon_c}^{\varepsilon_c} d\varepsilon \phi(\varepsilon) \frac{\Delta_\beta}{\varepsilon} \\
&= 2\pi T \sum_\beta \lambda_{\alpha\beta} \sum_{n=0}^{\infty} \Big[\langle f_\beta(\varepsilon_n, \mathbf{k}_{\rm F}) \rangle - \frac{\Delta_\beta}{\varepsilon_n} \Big] \\
&\quad + \sum_\beta \lambda_{\alpha\beta} \Delta_\beta \ln\left(\frac{2e^\gamma}{\pi} \frac{\varepsilon_c}{T} \right) \,,
\end{aligned} \tag{7}$$

where $\gamma = 0.577$ is the Euler constant, $\varepsilon_n \equiv (2n+1)\pi T$ is the Matsubara frequency, and $f_\alpha(\varepsilon_n) = f_\alpha^{\rm R}(i\varepsilon_n)$. The limit $\varepsilon_c \to \infty$ has been taken safely in the first integral to transform the integration into the summation over Matsubara frequencies. Equation (7) tells us that Δ_α has no angular dependence within the band. It then follows that f_α neither has any angular dependence, so that $\langle f_\alpha \rangle = f_\alpha$ and $\langle g_\alpha \rangle = g_\alpha$. Hence Eq. (1) with $\varepsilon \to i\varepsilon_n$ is simplified into

$$\left(\varepsilon_n + \frac{g_\beta}{2\tau_{\alpha\beta}} \right) f_\alpha = \left(\Delta_\alpha + \frac{f_\beta}{2\tau_{\alpha\beta}} \right) g_\alpha \qquad (\beta \neq \alpha) \,. \tag{8}$$

Thus, the intraband scattering does not affect superconductivity in zero magnetic field at all, in agreement with Anderson's theorem.[20] Equation (8) could be presented at the beginning in place of Eq. (1). However, Eqs. (1)-(3) have an advantage that they could easily be extended to nonuniform systems by simply adding gradient terms.[26,28]

Equations (7) and (8) enable us to obtain Δ_α from calculations on Matsubara frequencies, which are numerically more stable than Eqs. (1) and (2). Once Δ_α is fixed in this way, the density of states is calculated by solving Eq. (1) as

$$N(\epsilon) = \sum_\alpha N_\alpha(0) {\rm Re} g_\alpha^{\rm R}(\epsilon) \,. \tag{9}$$

B. Transition temperature

We now derive the T_c equation valid at all impurity concentrations. To this end, we expand f_α and g_α up to first order in Δ_β as $f_\alpha = f_\alpha^{(1)}$ and $g_\alpha = 1$. Substituting

them into Eq. (8), we obtain $f_\alpha^{(1)}$ as

$$f_\alpha^{(1)} = \sum_\beta h_{\alpha\beta}\Delta_\beta\,, \tag{10}$$

where $h_{\alpha\beta}$ is defined by

$$h_{\alpha\beta} = \delta_{\alpha\beta}\left(\frac{n_\alpha}{\varepsilon_n} + \frac{1-n_\alpha}{\varepsilon_n+\frac{1}{\tau}}\right) + (1-\delta_{\alpha\beta})\left(\frac{n_\beta}{\varepsilon_n} - \frac{n_\beta}{\varepsilon_n+\frac{1}{\tau}}\right), \tag{11}$$

with

$$n_\alpha \equiv \frac{N_\alpha(0)}{N_\alpha(0)+N_\beta(0)}\,, \qquad \frac{1}{\tau} \equiv \frac{1}{2\tau_{\alpha\beta}} + \frac{1}{2\tau_{\beta\alpha}}\,. \tag{12}$$

Substituting Eq. (10) into Eq. (7), we obtain the condition for a nontrivial solution as

$$\det[\mathbf{1} - H] = 0\,, \tag{13}$$

where the matrix H is defined by

$$H_{\alpha\beta} = \sum_\gamma \lambda_{\alpha\gamma}\left\{2\pi T_c \sum_{n=0}^{\infty}\left[h_{\gamma\beta}(\varepsilon_n) - \frac{\delta_{\gamma\beta}}{\varepsilon_n}\right] + \delta_{\gamma\beta}\ln\left(\frac{2e^\gamma}{\pi}\frac{\varepsilon_c}{T_c}\right)\right\}. \tag{14}$$

By solving Eq. (13), T_c is obtained for an arbitrary τ. Notice that all the summations in Eq. (14) can be expressed in terms of the digamma function $\psi(x)$.

When $T_c\tau \ll 1$, Eq. (13) can be solved explicitly by using the asymptotic expression $\psi(x)\sim\ln x$ $(x\to\infty)$ as

$$T_c = \frac{2e^\gamma}{\pi}\varepsilon_c \exp\left[\frac{\sum_{\alpha(\neq\beta)}(\lambda_{\alpha\beta}n_\alpha - \lambda_{\alpha\alpha}n_\beta)\ln(\varepsilon_c\tau)+1}{(\lambda_{\sigma\sigma}\lambda_{\pi\pi}-\lambda_{\sigma\pi}\lambda_{\pi\sigma})\ln(\varepsilon_c\tau) - \sum_\alpha \lambda_\alpha n_\alpha}\right]. \tag{15}$$

with $\lambda_\alpha \equiv \sum_\beta \lambda_{\alpha\beta}$. This expression is useful to see whether T_c is suppressed completely or not as the interband scattering increases.

C. Density of states in the dirty limit

We now derive an analytic expression for the density of states in the dirty limit of $T_c\tau \ll 1$. In this case with $\varepsilon \lesssim T_c$, we can neglect the first terms on both sides of Eq. (1). It then follows that $f_\alpha^{\rm R}/g_\alpha^{\rm R} = f_\beta^{\rm R}/g_\beta^{\rm R}$, or equivalently, $f_\alpha^{\rm R} = f_\beta^{\rm R} \equiv f^{\rm R}$ and $g_\alpha^{\rm R} = g_\beta^{\rm R} \equiv g^{\rm R}$. The quantities $f^{\rm R}$ and $g^{\rm R}$ are obtained easily as

$$f^{\rm R}(\varepsilon) = \frac{\bar\Delta}{\sqrt{\bar\Delta^2 - \varepsilon_+^2}}\,, \qquad g^{\rm R}(\varepsilon) = \frac{-i\varepsilon}{\sqrt{\bar\Delta^2 - \varepsilon_+^2}}\,, \tag{16}$$

where $\varepsilon_+ \equiv \varepsilon + i0_+$, and $\bar\Delta$ is defined by

$$\bar\Delta \equiv n_\sigma\Delta_\sigma + n_\pi\Delta_\pi\,. \tag{17}$$

TABLE I: Coupling constants

	$\lambda_{\sigma\sigma}$	$\lambda_{\sigma\pi}$	$\lambda_{\pi\sigma}$	$\lambda_{\pi\pi}$
Case A	2.45×10^{-1}	5.95×10^{-2}	4.28×10^{-2}	1.10×10^{-1}
Case B	2.25×10^{-1}	2.35×10^{-1}	1.69×10^{-1}	-1.22×10^{-1}

It hence follows that the density of states $\propto {\rm Re}\, g^{\rm R}$ has the conventional BCS structure, diverging at $\varepsilon = \pm\bar\Delta$. The corresponding pair potential is determined by

$$\Delta_\alpha = \frac{\lambda_\alpha}{2i}\int_{-\varepsilon_c}^{\varepsilon_c} d\varepsilon\phi(\varepsilon)f^{\rm R}(\varepsilon)\,, \tag{18}$$

as already pointed out by Golubov and Mazin.[23] Thus, the ratio of the two pair potentials is given by $\Delta_\sigma/\Delta_\pi = \lambda_\sigma/\lambda_\pi$.

D. Numerical procedures

There are five parameters in the model:

$$\lambda_{\sigma\sigma},\quad \lambda_{\sigma\pi},\quad \lambda_{\pi\pi},\quad \varepsilon_c,\quad N_\sigma(0)/N_\pi(0). \tag{19}$$

They are fixed so as to reproduce experiments on MgB_2 as closely as possible. To be more specific, the ratio $N_\sigma(0)/N_\pi(0)$ is set equal to 0.72 following an electronic-structure calculation.[32] As for the coupling constants, we use Eq. (2) in the clean limit at $T=0$, T_c which yields

$$1 = \lambda_{\sigma\sigma}\ln\left(\frac{2\varepsilon_c}{\Delta_\sigma}\right) + \lambda_{\sigma\pi}\frac{\Delta_\pi}{\Delta_\sigma}\left[\ln\left(\frac{2\varepsilon_c}{\Delta_\sigma}\right) - \ln\left(\frac{\Delta_\pi}{\Delta_\sigma}\right)\right], \tag{20a}$$

$$\frac{\Delta_\pi}{\Delta_\sigma} = \lambda_{\pi\sigma}\ln\left(\frac{2\varepsilon_c}{\Delta_\sigma}\right) + \lambda_{\pi\pi}\frac{\Delta_\pi}{\Delta_\sigma}\left[\ln\left(\frac{2\varepsilon_c}{\Delta_\sigma}\right) - \ln\left(\frac{\Delta_\pi}{\Delta_\sigma}\right)\right], \tag{20b}$$

and

$$\ln\left(\frac{2{\rm e}^\gamma\varepsilon_c}{\pi T_c}\right) = \frac{\lambda_{\sigma\sigma}+\lambda_{\pi\pi}+\sqrt{(\lambda_{\sigma\sigma}-\lambda_{\pi\pi})^2+4\lambda_{\sigma\pi}\lambda_{\pi\sigma}}}{2(\lambda_{\sigma\sigma}\lambda_{\pi\pi}-\lambda_{\sigma\pi}\lambda_{\pi\sigma})}\,, \tag{20c}$$

respectively. These equations are used to eliminate $\lambda_{\alpha\beta}$ in favor of $\Delta_{\sigma0}/\Delta_{\pi0}$, $T_c/\Delta_{\sigma0}$, and $\varepsilon_c/\Delta_{\sigma0}$, where $\Delta_{\sigma0,\pi0}$ denotes $\Delta_{\sigma,\pi}(T=0)$ in the clean limit.

We here consider the following two cases:[7,9,11,13]

$$\text{Case A}: \ \frac{T_c}{\Delta_{\sigma0}} = 0.50;\ \ \frac{\Delta_{\sigma0}}{\Delta_{\pi0}} = 3.00;\ \ \frac{\varepsilon_c}{\Delta_{\sigma0}} = 20.0, \tag{21a}$$

$$\text{Case B}: \ \frac{T_c}{\Delta_{\sigma0}} = 0.48;\ \ \frac{\Delta_{\sigma0}}{\Delta_{\pi0}} = 2.95;\ \ \frac{\varepsilon_c}{\Delta_{\sigma0}} = 10.0. \tag{21b}$$

These values are chosen so as to reproduce temperature dependence of the observed energy gaps on clean

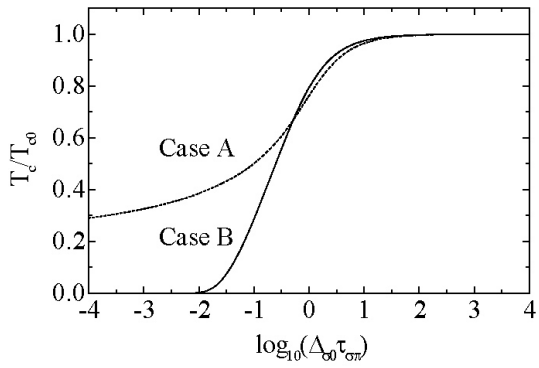

FIG. 1: Transition temperature as a function of $\log_{10}(\Delta_{\sigma 0}\tau_{\sigma\pi})$

samples[14,15,16,18] as closely as possible. The corresponding coupling constants are listed in Table I. It has been found that the whole results are rather insensitive to ε_c, as may be expected.

Numerical calculations have been performed as follows. First, f_α and g_α with $f_\alpha^2+g_\alpha^2=1$ are expressed conveniently in terms of a single function a_α as[29,30]

$$f_\alpha = \frac{2a_\alpha}{1+a_\alpha^2}, \qquad g_\alpha = \frac{1-a_\alpha^2}{1+a_\alpha^2}\,. \tag{22}$$

Substituting Eq. (22) and a trial $(\Delta_\sigma, \Delta_\pi)$ into it, Eq. (8) is transformed into a set of nonlinear equations for a_α, which may be solved by using one of the standard numerical procedures.[31] The obtained f_α is then substituted into Eq. (7) to find a new $(\Delta_\sigma, \Delta_\pi)$. This procedure is repeated until the convergence is reached. The pair potentials thereby obtained are then used in Eq. (1) to calculate $f^{\rm R}$ and $g^{\rm R}$ on the real energy axis. Finally, those $f^{\rm R}$ and $g^{\rm R}$ are substituted into Eqs. (5), (6), and (9) to calculate the specific heat and the density of states.

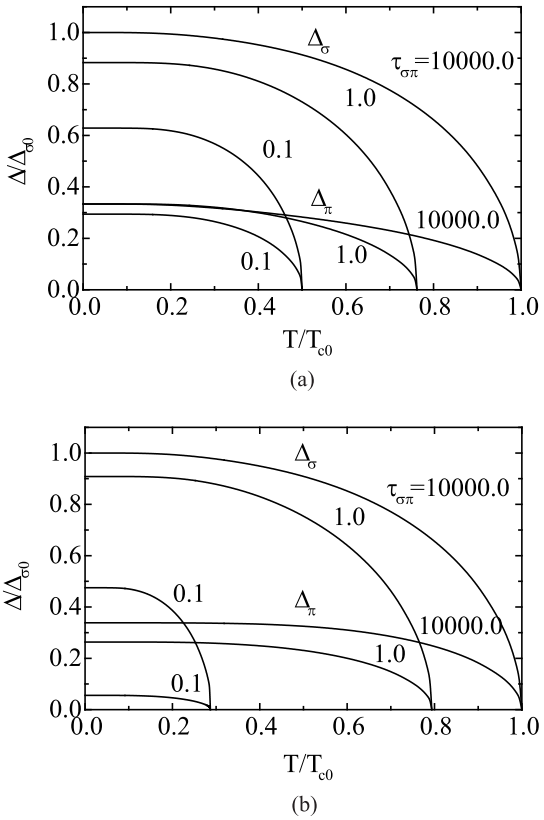

FIG. 2: The pair potentials as a function of T/T_{c0} for three different impurity concentrations. (a) Case A; (b) Case B. Here $\tau_{\sigma\pi}$ is given in units of $\Delta_{\sigma 0}^{-1}$

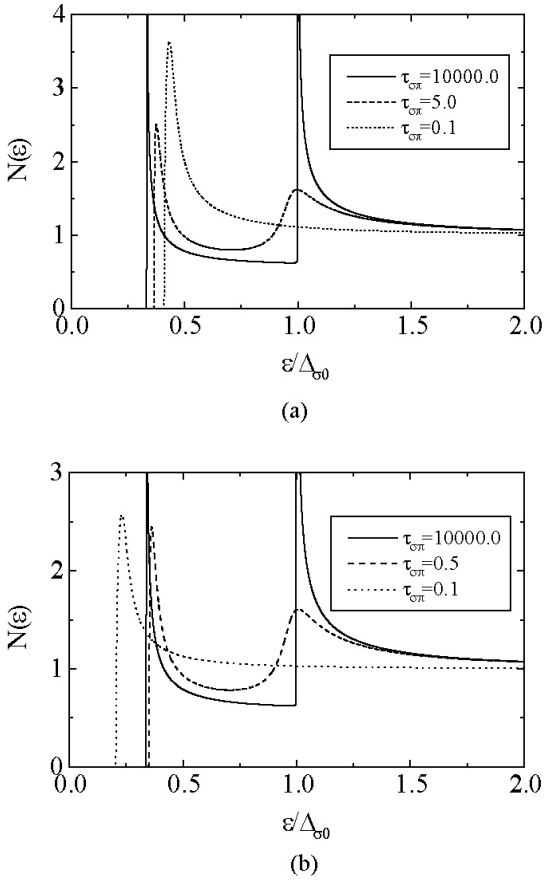

FIG. 3: Density of states at $T = 0.01T_c$ for three different $\tau_{\sigma\pi}$. (a) Case A; (b) Case B. Here $\tau_{\sigma\pi}$ is given in units of $\Delta_{\sigma 0}^{-1}$

III. RESULTS

Figure 1 plots T_c as a function of the interband scattering specified by $\log_{10}(\Delta_{\sigma 0}\tau_{\sigma\pi})$ for the two cases of Eq. (21). Here T_c is normalized by T_{c0} without the interband

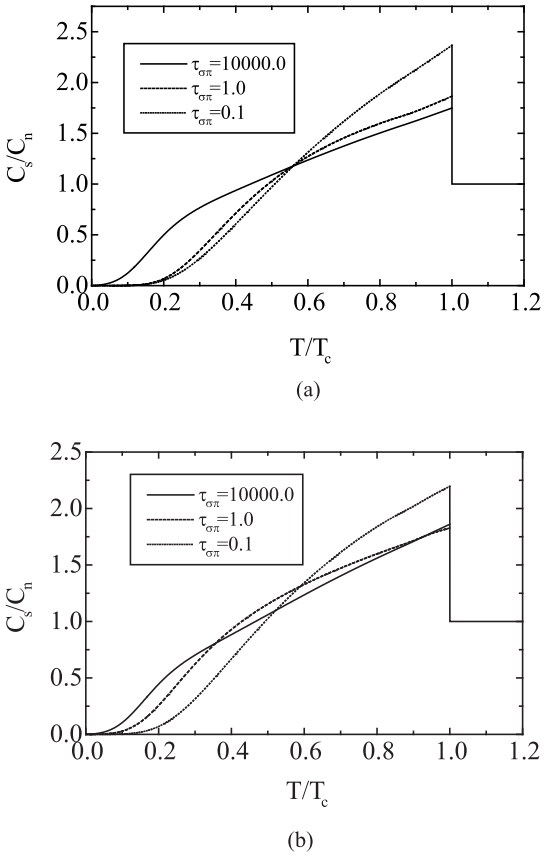

FIG. 4: Specific heat as a function of T/T_c for $\tau_{\sigma\pi}=10000.0$, 1.0, and 0.1. (a) Case A; (b) Case B. Here $\tau_{\sigma\pi}$ is given in units of $\Delta_{\sigma 0}^{-1}$

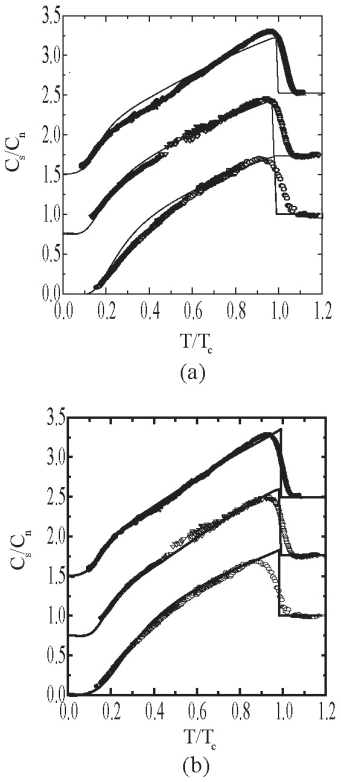

FIG. 5: Comparisons of theoretical curves with specific-heat measurements before irradiation (top), after the first irradiation (middle), and after the second irradiation (bottom) of Ref. 13. (a) Case A with $\Delta_{\sigma 0}\tau_{\sigma\pi}=50.0$, 7.0, 4.0 from top to bottom. (b) Case B $\Delta_{\sigma 0}\tau_{\sigma\pi}=10000.0$, 30.0, 1.0 from top to bottom.

scattering. We observe that T_c drops steeply around $\tau_{\sigma\pi}=\Delta_{\sigma 0}^{-1}$ in both cases. However, whereas T_c in Case A remains finite for $\tau_{\sigma\pi}\to 0$, T_c in Case B decreases to zero at a finite $\tau_{\sigma\pi}$. This difference can be realized from Eq. (15) where the term in the square bracket passes through negative infinity for $T_c\to 0$. It is interesting to see experimentally whether T_c of MgB_2 is suppressed completely or not by increasing the interband scattering, although this may not be easy.[25]

Figure 2 shows temperature dependence of the pair potentials for (a) Case A and (b) Case B. In both cases, the pair potentials decrease as $\tau_{\sigma\pi}$ becomes shorter. However, the two pair potentials do not approach to a single value even for $\tau_{\sigma\pi}\to 0$. Notice also that the pair potentials are not directly connected with any observable quantities except in the clean limit.

Figure 3 shows the density of states at $T/T_c=0.01$ for (a) Case A and (b) Case B. In the clean limit $\Delta_{\sigma 0}\tau_{\sigma\pi}=10000.0$, we clearly observe a couple of divergences at $\varepsilon=\Delta_\sigma$, Δ_π. As the interband scattering becomes larger, the divergences are smeared to finite peaks, which eventually merge into a single peak in the dirty limit at $\varepsilon=\bar{\Delta}$ given by Eq. (17). Notice that the excitation threshold is not a monotonic function of $\tau_{\sigma\pi}$; for Case A, for example, the threshold is seen to increase as $\tau_{\sigma\pi}$ becomes smaller.

Figure 4 plots the specific heat as a function of T/T_c in (a) Case A and (b) Case B for $\Delta_{\sigma 0}\tau_{\sigma\pi}=10000.0$, 1.0, 0.1. A shoulder is clearly seen around $T/T_c=0.2$ for $\Delta_{\sigma 0}\tau_{\sigma\pi}=10000.0$, corresponding to the divergence at $\varepsilon=\Delta_\pi$ in Fig.3. It gradually disappears as $\tau_{\sigma\pi}$ becomes shorter, however, and we finally have a conventional single-exponential behavior in the dirty limit.

Finally, Fig. 5 compares the present theory with the specific-heat experiment after irradiation performed by Wang *et al.*[13] The data points correspond to measurements before irradiation (top), after the first irradiation (middle), and after the second irradiation (bottom), where the former two are shifted upwards by $1.5C_n$ and $0.75C_n$, respectively. The curves of Fig. 5(a) are obtained by using the parameters of Case A with $\Delta_{\sigma 0}\tau_{\sigma\pi}=50.0$, 7.0, 4.0 from top to bottom, respectively. On the other hand, those of Fig. 5(b) correspond to Case B with $\Delta_{\sigma 0}\tau_{\sigma\pi}=10000.0$, 30.0, 1.0. The agreements are good

for both cases, especially for Case B. From these comparisons, we realize that the interband scattering after the second irradiation is still not very strong with $\Delta_{\sigma 0}\tau_{\sigma\pi} \gtrsim 1.0$. The fact may imply the difficulty of introducing the interband impurity scattering in MgB_2.[25] This tendency is also seen in the carbon-substituted system $Mg(B_{1-x}C_x)_2$ where the two-gap structure is still observed clearly for $x \sim 0.1$.[33] Thus, the large reduction of T_c observed in $Mg(B_{1-x}C_x)_2$ by Lee *et al.*[24] should be attributed not only to the interband scattering alone but also to a change of the pairing interaction due to the electronic structure.

IV. CONCLUSION

We have studied nonmagnetic impurity effects for MgB_2 based on the quasiclassical equations of superconductivity for the Suhl-Matthias-Walker model. The parameters in the model are fixed so as to reproduce experimental values for $\Delta_{\pi 0}/\Delta_{\sigma 0}$ and $\Delta_{\sigma 0}/T_c$. The interband impurity scattering tends to reduce the gap anisotropy. We have clarified how the density of states changes from the two-gap structure in the clean limit to the single-gap structure in the dirty limit with strong interband scattering. Especially, there may be cases where the excitation threshold increases as the scattering becomes stronger. Calculated curves for the specific heat agree well with measurements before and after irradiation. This comparison has also enabled us to estimate the relaxation time $\tau_{\sigma\pi}$ for the interband scattering. It satisfies $\tau_{\sigma\pi} \gtrsim 1/\Delta_{\sigma 0}$ even after the second irradiation, implying the difficulty of introducing the interband scattering in this system.

Acknowledgments

This work is supported by a Grant-in-Aid for Scientific Research from the Ministry of Education, Culture, Sports, Science, and Technology of Japan.

[1] J. Nagamatsu, N. Nakagawa, T. Muranaka, Y. Zenitani, and J. Akimitsu, Nature **410**, 63 (2001).

[2] S.L. Bud'ko, G. Lapertot, C. Petrovic, C.E. Cunningham, N. Anderson, and P.C. Canfield, Phys. Rev. Lett. **86**, 1877 (2001).

[3] A.Y. Liu, I.I. Mazin, and J. Kortus, Phys. Rev. Lett. **87**, 087005 (2001).

[4] Y. Kong, O.V. Dolgov, O. Jepsen, O.K. Andersen, Phys. Rev. B **64**, 020501 (2001).

[5] H.J. Choi, D. Roundy, H. Sun, M.L. Cohen, and S.G. Louie, Phys. Rev. B **66**, 020513 (2002); Nature **418**, 758 (2002).

[6] I.I. Mazin and V.P. Antropov, Physica C **385**, 49 (2003).

[7] Y. Wang, T. Plackowski, and A. Junod, Pysica C **355**, 179 (2001).

[8] F. Bouquet, R.A. Fisher, N.E. Phillips, D.G. Hinks, and J.D. Jorgensen, Phys. Rev. Lett. **87**, 047001 (2001).

[9] H.D. Yang, J.-Y. Lin, H.H. Li, F.H. Hsu, C.J. Liu, S.-C. Li, R.-C. Yu, and C.-Q. Jin, Phys. Rev. Lett. **87**, 167003 (2001).

[10] F. Bouquet, Y. Wang, I. Sheikin, T. Plackowski, A. Junod, S. Lee, and S. Tajima, Phys. Rev. Lett. **89**, 257001 (2002).

[11] F. Bouquet, Y. Wang, R.A. Fisher, D.G. Hinks, J.D. Jorgensen, A. Junod, and N.E. Phillips, Europhys. Lett. **56**, 856 (2001).

[12] A.A. Golubov, J. Kortus, O.V. Dolgov, O. Jepsen, Y. Kong, O.K. Andersen, B.J. Gibson, K. Ahn, and R.K. Kremer, J. Phys. Condens. Matter **14**, 1353 (2002).

[13] Y. Wang, F. Bouquet, I. Sheikin, P. Toulemonde, B. Revaz, M. Eisterer, H.W. Weber, J. Hinderer, and A. Junod, J. Phys. Condens. Matter **15**, 883 (2003).

[14] P. Szabó, P. Samuely, J. Kačmarčík, T. Klein, J. Marcus, D. Fruchart, S. Miraglia, C. Marcenat, and A.G.M. Jansen, Phys. Rev. Lett. **87**, 137005 (2001).

[15] H. Schmidt, J.F. Zasadzinski, K.E. Gray, and D.G. Hinks, Phys. Rev. Lett. **88**, 127002 (2001).

[16] R.S. Gonnelli, D. Daghero, G.A. Ummarino, V.A. Stepanov, J. Jun, S.M. Kazakov, and J. Karpinski, Phys. Rev. Lett. **89**, 247004 (2002).

[17] F. Giubileo, D. Roditchev, W. Sacks, R. Lamy, D.X. Thanh, J. Klein, S. Miraglia, D. Fruchart, J. Marcus, and Ph. Monod, Phys. Rev. Lett. **87**, 177008 (2001).

[18] M. Iavarone, G. Karapetrov, A.E. Koshelev, W.K. Kwok, G.W. Crabtree, D.G. Hinks, W.N. Kang, E.-M Choi, H.J. Kim, H.-J. Kim, and S.I. Lee, Phys. Rev. Lett. **89**, 187002 (2002).

[19] M.R. Eskildsen, M. Kugler, S. Tanaka, J. Jun, S.M. Kazakov, J. Karpinski, and O. Fischer, Phys. Rev. Lett. **89**, 187003 (2002).

[20] P.W. Anderson, J. Phys. Chem. Solids **11**, 26 (1959).

[21] A.A. Abrikosov and L.P. Gor'kov, Zh. Eksp. Teor. Fiz. **35**, 1558 (1958)

[22] D. Markowitz and L.P. Kadanoff, Phys. Rev. **131**, 563 (1963). [Sov. Phys. JETP **8**, 1090 (1959)].

[23] A.A. Golubov, and I.I. Mazin, Phys. Rev. B **55**, 15146 (1997).

[24] S. Lee, T. Masui, A. Yamamoto, H. Uchiyama, and S. Tajima, Physica C **397**, 7 (2003).

[25] I.I. Mazin, O.K. Andersen, O. Jepsen, O.V. Dolgov, J. Kortus, A.A. Golubov, A.B. Kuz'menko, and D. van der Marel, Phys. Rev. Lett. **89**, 107002 (2002).

[26] G. Eilenberger, Z. Phys. **214**, 195 (1968).

[27] H. Suhl, B.T. Matthias, and L.R. Walker, Phys. Rev. Lett. **3**, 552 (1959).

[28] T. Kita, Phys. Rev. B **68**, 184503 (2003).

[29] N. Schopohl and K. Maki, Phys. Rev. B **52**, 490 (1995).

[30] Y. Nagato, K. Nagai, and J. Hara, J. Low Temp. Phys. **93**, 33 (1993); Y. Nagato, S. Higashitani, K. Yamada, and K. Nagai, J. Low Temp. Phys. **103**, 1 (1996).

[31] W.H. Press, S.A. Teukolsky, W.T. Vetterling, and B.P. Flannery, *Numerical Recipes in C* (Cambridge University Press, Cambridge, 1988).

[32] K.D. Belashchenko, V.P. Antropov, and S.N. Rashkeev, Phys. Rev. B **64**, 132506 (2001).

[33] A. Shibata, M. Matsumoto, K. Izawa, and Y. Matsuda, private communications.